Oxygen transfer centers in Fe-FER and Fe-MFI zeolites: redox behavior and Debye temperature derived from *in situ* Mössbauer spectra

Károly Lázár [a,*], A.N. Kotasthane [b] and Pál Fejes [c]

[a] *Institute of Isotope and Surface Chemistry, PO Box 77, H-1525 Budapest, Hungary*
E-mail: lazar@iserv.iki.kfki.hu
[b] *United Catalysts India, Ltd., Nandesari 391 340, India*
[c] *Department of Applied Chemistry, József Attila University, H-6720 Szeged, Hungary*

Received 14 September 1998; accepted 11 January 1999

77 and 300 K *in situ* Mössbauer spectra recorded after redox treatments of Fe-FER and Fe-MFI ferrisilicates are compared. Similar behavior is found for the two catalysts; reversible redox processes can be detected. Oxidation and coordination states are identified after various treatments, and the value of the average Debye temperature is estimated ($260 < \Theta_D < 300$ K). Analysis and comparison of data support the assignment of redox centers to $Fe_{framework}$–O–$Fe_{extra\text{-}framework}$ pairs.

Keywords: ferrisilicates, Fe–O–Fe centers, redox behavior, Mössbauer spectroscopy

1. Introduction

Fe-MFI zeolites have recently seen renewed interest due to their ability to catalyse selective oxidation reactions in diverse fields. An important application is selective catalytic reduction (SCR) in deNOx processes, where the ferrisilicates are stable and are capable of withstanding water vapor [1–6]. Another promising use is the activation of oxygen to form the particularly reactive (so called α-) oxygen: activation of Fe-MFI by N_2O results in a catalyst which is able to oxidize benzene to phenol at room temperature [7,8]. Such zeolites can also be used in more conventional processes, e.g., in oxidative dehydrogenation of alkanes [9]. Reports on Fe-FER are scarce although it has a very similar structure to Fe-MFI [10]. An application has recently been reported describing the selective oxidation of n-hexane using H_2O_2 in acetonitrile medium [11].

A particular feature of these ferrisilicate catalysts is that they can be prepared by various methods, e.g., by conventional aqueous ion exchange of H-MFI [1,2], by evaporating $FeCl_3$ into cavities of H-MFI [3,4], or by solid-state ion exchange in mixtures of NH_4-MFI and $FeCl_2$ [5]. Framework-substituted Fe-MFI and Fe-FER also exhibit excellent catalytic properties [6–9,11]; in fact, comparative studies showed the latter to be superior to the ion-exchanged catalysts [6,9].

There is general agreement that the catalytic activity is linked with the presence of iron, however, there are various suggestions as to the form and the location of this active species. In most of the explanations dinuclear iron centers are suggested, but it has also been reported that an oligonuclear center might be responsible [12]. As for the location and bonding of the dinuclear species, various possibilities have been put forward. For example, extra-framework emplacement can be suggested for the Fe–O–Fe in analogy to iron-exchanged Y zeolites which also catalyse the SCR of NO [13]. Another interpretation is that bonding of the Fe–O–Fe center to the framework takes place via a second oxygen bridge [4]. A further variation has recently been put forward based on the redox behavior observed in Fe-FER catalysts: a combined dinuclear $Fe_{framework}$–O–$F_{extra\text{-}framework}$ center [14]. In the formation of the Fe–O–Fe pairs further processes may also take part, e.g., the $Fe^{3+} \rightarrow Fe^{2+}$ autoreduction, which process can take place upon simple heating in vacuum and is accompanied by removal of framework-substituted ions [15]. The redox process itself may also change the position of ions of transient metals in zeolites [16].

In situ Mössbauer spectroscopy may contribute to the identification and characterization of the iron species even directly under the treating and reaction conditions of zeolites, since the oxidation and coordination states of iron ions can directly be derived from the spectra. The relevant information is primarily obtained from the isomer shift (IS) and quadrupole splitting (QS) values. The value of another parameter, the Debye temperature, Θ_D, can also be determined from the spectra. The Θ_D value characterizes the bonding strength of the Mössbauer active nucleus to its environment: the stronger the bond, the larger the Θ_D. For the determination of Θ_D, the resonant absorption area (RAA) values should first be determined as a function of temperature and then, in turn, the Θ_D values can be obtained [17,18]. The change of RAA upon adsorption of water in

* To whom correspondence should be addressed.

zeolites was demonstrated in [19]. The bonding strength of ionic centers in tin-zeolite catalysts used for oxygen transfer were recently characterized by determining the change of their RAA values [20]; to the best of our knowledge similar *in situ* studies on iron zeolites by estimating Θ_D have not been published.

In our preliminary publication, redox behavior was demonstrated in a Fe-FER oxygenation catalyst and this feature was attributed to a reversible $Fe^{3+} \leftrightarrow Fe^{2+}$ change taking place on both iron ions of the dinuclear $Fe_{framework}$–O–$Fe_{extra\text{-}framework}$ centers [14]. In the present work, Fe-FER is compared with Fe-MFI, and similar behavior is observed for both ferrisilicates; in addition, average Θ_D values are estimated for both catalysts. Analysis and comparison of data provide further support for the suggested assignment and position of the redox Fe–O–Fe centers.

2. Experimental

The Fe-FER sample used in the experiments was synthesized hydrothermally with a Si/Fe ratio of 16 using a pyrrolidine template. After synthesis the sample was dried and calcined stepwise up to 750 K. The sample contains the iron in framework-substituted position in a large proportion. Further details of synthesis and characterization are described in [11]. This Fe-FER exhibits favorable activity in partial oxidation of n-hexane to hexanone and in hydroxylation of phenol to catechol and hydroquinone using H_2O_2 in acetonitrile medium [14].

The Fe-MFI sample was also synthesized hydrothermally, by a sol–gel technique using tetrapropylammonium hydroxide as the template; the Si/Fe ratio is 15. Further details of the synthesis are described in [21]. The sample was calcined at 970 K, which slightly damaged the framework and led to the partial transference of iron to extra-framework positions [22].

The further treatments were performed in the *in situ* Mössbauer cell. Fe-FER was treated at a slightly higher temperature (at 620 K) since it contained a greater part of its iron in the framework-substituted position. Taking into account the higher percentage of the extra-framework iron in Fe-MFI, this sample was treated at a slightly lower temperature – at 570 K. Two types of treatments were applied (both for 2 h): evacuation (10^{-1} Pa) and hydrogen treatment in a flow of purified hydrogen (1 bar, 2 ml/min). The treatments resulted in 5 and 7 wt% weight losses of the Fe-MFI and Fe-FER samples, respectively, which losses are attributed to removal of the adsorbed water.

Subsequent *in situ* Mössbauer spectra were recorded after each treatment, step by step, at 77 and 300 K on the same sample. A Lorentzian line-shape is assumed for the components, and positional parameters were not constrained in the fitting procedure. Isomer shift values are related to α-iron, the relative resonant absorption area (RAA) values are related to the respective base line. The accuracy of positional parameters is ca. ± 0.03 mm/s.

3. Results

Prior to giving a detailed description and evaluation of the spectra it should be mentioned that the assignments of the coordinations for the various iron species are approximate ones. In general, only two markedly different coordinations are distinguished: the octahedral (Oh) and the tetrahedral (Td). As a consequence, a slight variation may appear in the respective IS and QS data assigned to the same coordination state in the tables. A great variety of posssible coordinations exists for iron in silicates (see, e.g., in [23]). In zeolites, as a first approximation, the Fe^{3+}_{Td} ions can be considered as framework-substituted ones. The Fe^{3+}_{Oh} component may be assigned both to extra-framework species or to framework-substituted ones, to which water molecules are adsorbed. The hydrogen treatment usually provides a means of separating the framework-substituted iron from the extra-framework one, the latter is easier to reduce. In addition, a further distinction is possible for the framework-substituted Fe^{3+}_{Td} component, depending on the counterion. After removing the water from the Si–O–Fe(OH)–O–Si Brønsted acidic sites, the remaining proton

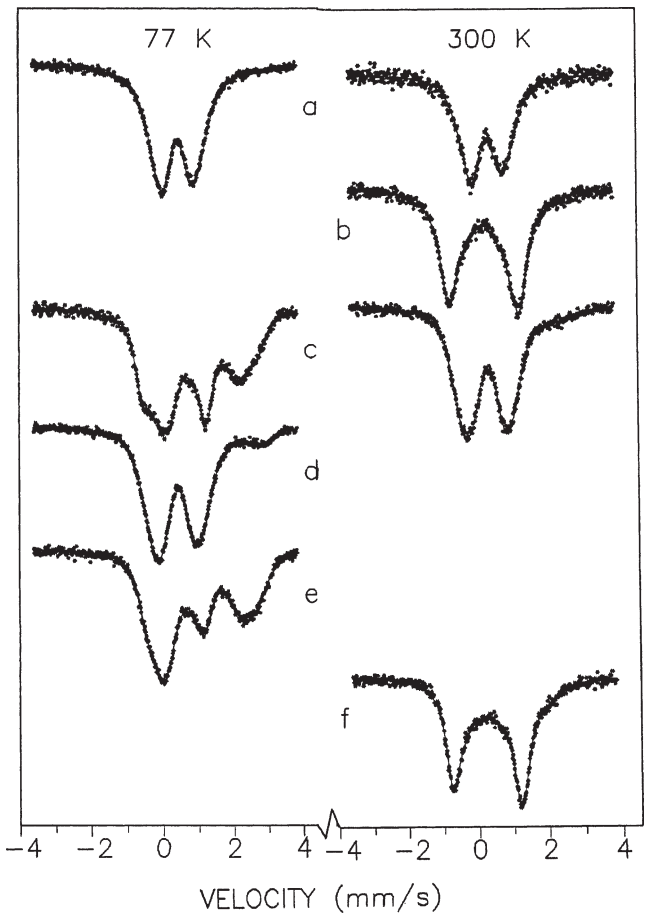

Figure 1. 77 and 300 K *in situ* Mössbauer spectra recorded on the Fe-FER sample after sequential treatments: (a) as received (synthesized and calcined), (b) evacuated at 620 K (10^{-1} Pa), (c) reduced in hydrogen at 620 K, (d) repetition of the 77 K measurement (77 → 300 → 77 K cycle), (e) repetition of the 620 K reduction in hydrogen, (f) repetition of evacuation at 620 K.

introduces large asymmetry which is reflected in the large (>1.7 mm/s) QS values (marked as $Fe^{3+}_{Td,2}$ coordination). In the case of other counterions, usually smaller QS values can be detected (1.3 < QS < 1.6 mm/s); this species is referred to as $Fe^{3+}_{Td,1}$ [24–26].

3.1. Fe-FER sample

Subsequent spectra obtained after various treatments of the Fe-FER sample are presented in figure 1, and the corresponding data derived are collected in table 1. The first treatment, evacuation, results in a noticeable change: the large quadrupole doublet characteristic of the $Fe^{3+}_{Td,2}$ appears as a major component (figure 1(b)). This can be attributed to the removal of the adsorbed water (as was mentioned before). The second treatment, in hydrogen results in $Fe^{3+} \rightarrow Fe^{2+}$ reduction to a considerable extent: in the 77 K spectrum recorded immediately after the treatment, ca. 50% Fe^{2+} component is detected (figure 1(c)). The moderate rise of the measuring temperature (from 77 to 300 K) results in a significant increase in the proportion of Fe^{3+} at the expense of the Fe^{2+} contribution. This change can be attributed to the reversible redox change taking place in the $Fe_{framework}$–O–$Fe_{extra\text{-}framework}$ centers, as suggested and described in [14]. A certain amount of iron is still preserved in the Fe^{2+} state (8% spectral area in the 300 K spectrum). Repetition of the measurement at 77 K results in a slight increase of the Fe^{2+} contribution (11% spectral area – figure 1(d)). (The increase of the Fe^{2+} contribution proves that the $Fe^{2+} \rightarrow Fe^{3+}$ oxidation shown previously in the spectrum of figure 1(c) immediately after the reduction cannot be attributed to oxidation by contamination or the leaking of air; in this particular case, the oxidation should continue during the measurement and further conversion of Fe^{2+} to Fe^{3+} would be detected.) Repetition of a reducing treatment in hydrogen at 620 K proves that the $Fe^{3+} \rightarrow Fe^{2+}$ redox cycle is reversible; a similar spectrum is recorded at 77 K (figure 1(e)) with a similar decomposition for components as found after the first reduction (in figure 1(c)). The structure of the Fe-FER sample is only slightly modified by the sequence of treatments applied; the main component in the spectrum recorded after a final evacuation is still the framework-substituted $Fe^{3+}_{Td,2}$ in the

Table 1
Data derived from 77 and 300 K *in situ* Mössbauer spectra of the Fe-FER sample.[a]

Treatment	Component[b]	77 K				300 K				$-\Delta f_A/\Delta T$[d]
		IS	QS	RI	RAA[c]	IS	QS	RI	RAA[c]	($\times 10^3$)
As received	Fe^{3+}_{Oh}	0.45	1.23	58	2.29	0.33	1.43	33	1.52	1.3
(calcined)	$Fe^{3+}_{Td/Oh}$					0.29	0.56	26		
	Fe^{3+}_{Oh}	0.42	0.73	42		0.36	0.96	40		
Evacuated,	$Fe^{3+}_{Td,2}$					0.24	1.98	71	1.58	
620 K	Fe^{3+}_{Oh}					0.37	1.17	29		
Hydrogen,	$Fe^{3+}_{Td,1}$	0.34	1.81	16	2.65	0.29	1.58	40	1.68	1.4
620 K	$Fe^{3+}_{Td/Oh}$	0.44	1.29	32		0.31	0.94	51		
	$Fe^{2+}_{Td/Oh}$	1.13	2.03	39		0.86	2.34	4		
	Fe^{2+}_{Oh}	1.43	2.46	12		1.31	2.44	4		
Hydrogen,	$Fe^{3+}_{Td,1}$	0.40	1.49	51	2.65					
300 K[e]	$Fe^{3+}_{Td/Oh}$	0.40	0.89	38						
	$Fe^{2+}_{Td/Oh}$	1.17	2.60	5						
	Fe^{2+}_{Oh}	1.52	2.85	6						
Hydrogen,	$Fe^{3+}_{Td,1}$	0.38	1.66	17	2.77					
620 K (repeat)	$Fe^{3+}_{Td/Oh}$	0.40	1.14	26						
	$Fe^{2+}_{Td/Oh}$	1.15	2.02	30						
	Fe^{2+}_{Oh}	1.32	2.65	27						
Evacuated,	$Fe^{3+}_{Td,2}$					0.20	1.98	60	1.76	1.4
620 K[f]	Fe^{3+}_{Oh}					0.47	1.91	25		
	Fe^{3+}_{Oh}					0.44	0.80	15		

[a] IS = isomer shift related to α-iron (mm/s); QS = quadrupole splitting (mm/s); RI = relative intensity (%); RAA = resonant absorption area (%).

[b] Approximate coordinations: Td = tetrahedral, Oh = octahedral; $Fe^{3+}_{Td,2}$ = framework substituted with H^+ counterion (protonated); $Fe^{3+}_{Td,1}$ = framework substituted with other counterions.

[c] Total value (sum from all the components).

[d] Calculated from the respective 77 and 300 K data: $(RAA_{300\ K} - RAA_{77\ K})/223$, and normalized corresponding to figure 1 in [18].

[e] Simple repetition of the previous 77 K measurement following the 300 K one.

[f] For estimating the $\Delta f_A/\Delta T$ slope the corresponding 77 K RAA value of the last hydrogen reduced spectrum (2.77) is considered.

Si–O–Fe(OH)–O–Si groups (the shapes of the spectra of figure 1 (b) and (f) are similar). However, the decomposition of spectra by fitting reveals that a slight modification of the distribution among the components has also taken place (table 1).

Comparison of the respective RAA (relative resonant absorption area) values of the spectra shows only a slight change in the sequence of treatments. The largest change is found after evacuation (which is probably related to the removal of water), but this change is only ca. 10%. The large change in the oxidation state resulting from the reduction (Fe^{2+} component appears in ca. 50% spectral area) is hardly reflected in the change of the corresponding RAA values. Thus, as it can be deduced, the strength of the bonding of iron ions did not change to any great extent by the reduction. (For example, not a large proportion of ions was removed from the framework, nor were they surrounded by water molecules.)

From comparison of the RAA values deduced from the spectra recorded at 300 and 77 K an estimate can also be given for the value of the Debye temperature (Θ_D). In a general case, the dependence of the recoilless fraction (f_A) on the measuring temperature is a complicated function [17]. However, in a certain interval ($250 < \Theta_D < 450$ K) the f_A–T dependence is close to linear in the 77–300 K range [18]. Thus, from the respective RAA values the $\Delta f_A/\Delta T$ slope and the respective Θ_D values can be estimated in this given region of Θ_D. These slopes are also calculated and are shown in table 1. The slope obtained is $-(1.3\text{–}1.4) \times 10^{-3}$ K^{-1}, corresponding to $\Theta_D \approx 260$ K. It should be mentioned that this value is a mean one since it is estimated from the change of the total spectral area. (The respective Θ_D values for the separate components could also be estimated, but the temperature-dependent redox changes would interfere with the intensity changes assigned to the separate components.)

3.2. Fe-MFI sample

The series of spectra recorded at 77 and 300 K after the various treaments of the Fe-MFI is shown in figure 2, the corresponding data extracted from the fits are collected in table 2.

The first treatment – evacuation at 570 K – resulted in a similar change to that experienced in the Fe-FER sample: a significant increase of the quadrupole splitting is found (attributed to the appearance of the Brønsted acidic O–SiO–Fe(OH)–OSi groups in the structure due to the removal of water from the larger hydroxonium ions [25]). It should be noted that an additional new feature, the appearance of an Fe^{2+} component, is also detected upon evacuation (with 14% spectral area – figure 2(b)). This latter process can probably be related to a slight $Fe^{3+} \rightarrow Fe^{2+}$ autoreduction that takes place with the participation of extra-framework iron ions [16].

On reducing the sample, behavior very similar to that of the previous Fe-FER sample was experienced: the treatment in hydrogen resulted in a significant increase of the Fe^{2+} component in the 77 K spectrum (to 37% spectral area – figure 2(c)). Upon increasing the temperature of measurement to 300 K the major part of the Fe^{2+} contribution was converted to Fe^{3+}. By the subsequent cooling to 77 K again the distribution of iron among the various coordinations was not changed (figure 2(d)). The redox process exhibited by the iron ions is reversible: a similar spectrum can be recorded after the second hydrogen treatment (figure 2(e)) as was obtained after the first reduction. Comparison of the corresponding data in table 2 shows that the Fe^{2+} contribution is slightly increased by repeating the reduction process (from 37 to 43% spectral area).

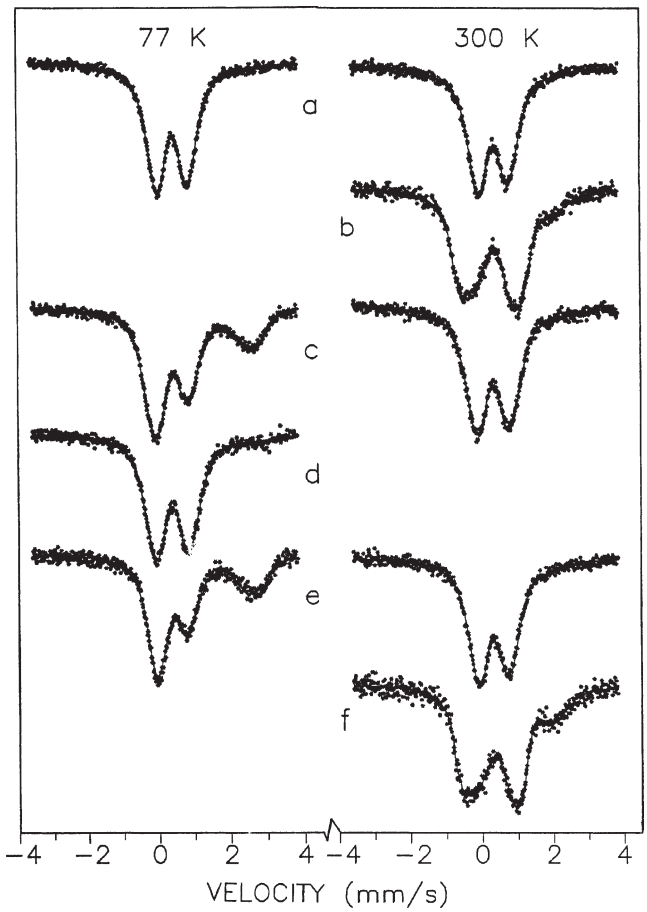

Figure 2. 77 and 300 K *in situ* Mössbauer spectra recorded on the Fe-MFI sample after sequential treatments: (a) as received (synthesized and calcined), (b) evacuated at 620 K (10^{-1} Pa), (c) reduced in hydrogen at 620 K, (d) repetition of the 77 K measurement (77 → 300 → 77 K cycle), (e) repetition of the 620 K reduction in hydrogen, (f) repetition of evacuation at 620 K.

Finally, evacuation was again applied at 570 K (figure 2(f)), the shape of the spectrum of the starting sample was almost restored (cf. figure 2(b)). The decomposition of the spectrum shows that the Fe^{2+} contribution is increased to 27% spectral area in the final state.

The corresponding relative resonant absorption area (RAA) values were also calculated from the spectra. The values calculated for 77 and 300 K show only a slight change upon the various treatments, similarly as was found

Table 2
Data derived from 77 and 300 K *in situ* Mössbauer spectra of the Fe-MFI sample.[a]

Treatment	Component[b]	77 K				300 K				$-\Delta f_A/\Delta T$[d]
		IS	QS	RI	RAA[c]	IS	QS	RI	RAA[c]	($\times 10^3$)
As received	$Fe^{3+}_{Td/Oh}$	0.41	1.05	68	1.19	0.33	0.85	100	0.85	1.2
(calcined)	Fe^{3+}_{Oh}	0.42	0.66	32						
Evacuated,	$Fe^{3+}_{Td,2}$					0.24	1.94	19	0.82	
570 K	$Fe^{3+}_{Td,1}$					0.26	1.51	34		
	Fe^{3+}_{Oh}					0.31	0.90	33		
	Fe^{2+}_{Oh}					1.10	1.88	14		
Hydrogen,	$Fe^{3+}_{Td/Oh}$	0.44	1.03	44	1.12	0.33	1.14	58	0.91	1.0
570 K	Fe^{3+}_{Oh}	0.40	0.60	19		0.31	0.67	36		
	$Fe^{2+}_{Td/Oh}$	1.09	2.45	20						
	Fe^{2+}_{Oh}	1.22	3.05	17		1.09	2.92	6		
Hydrogen,	$Fe^{3+}_{Td/Oh}$	0.40	1.20	48	1.20					
300 K[e]	Fe^{3+}_{Oh}	0.39	0.73	46						
	Fe^{2+}_{Oh}	1.27	3.09	7						
Hydrogen,	$Fe^{3+}_{Td/Oh}$	0.37	1.13	18	1.27	0.30	0.54	21	0.88	1.2
570 K (repeat)	Fe^{3+}_{Oh}	0.34	0.77	39		0.33	0.98	73		
	$Fe^{2+}_{Td/Oh}$	1.13	2.23	14		0.89	2.36	7		
	Fe^{2+}_{Oh}	1.38	2.70	29						
Evacuated,	$Fe^{3+}_{Td,2}$					0.21	1.89	4	0.82	
570 K	$Fe^{3+}_{Td,1}$					0.24	1.53	31		
	$Fe^{3+}_{Td/Oh}$					0.29	0.91	37		
	Fe^{2+}_{Oh}					1.05	1.96	27		

[a] IS = isomer shift related to α-iron (mm/s); QS = quadrupole splitting (mm/s); RI = relative intensity (%); RAA = resonant absorption area (%).

[b] Approximate coordinations: Td = tetrahedral; Oh = octahedral; $Fe^{3+}_{Td,2}$ = framework substituted with H^+ counterion (protonated); $Fe^{3+}_{Td,1}$ = framework substituted with other counterions.

[c] Total value (sum from all the components).

[d] Calculated from the respective 77 and 300 K data: $(RAA_{300\ K} - RAA_{77\ K})/223$, and normalized corresponding to figure 1 in [18].

[e] Simple repetition of the previous 77 K measurement following the 300 K one.

for the Fe-FER sample. The $\Delta f_A/\Delta T$ values were also determined. The values of this slope are slightly larger than those found for Fe-FER (correlated probably to the stabilizing effect of the starting high-temperature calcination). Again, it is worth mentioning that the variation of the treatments does not result in a significant change in the $\Delta f_A/\Delta T$ values, although a redox cycle has taken place meanwhile with the participation of a considerable portion of the iron ions. The values of the average Θ_D temperatures can also be estimated as was mentioned for the Fe-FER sample, a value of $\Theta_D \approx 280$–300 K can be estimated from the $-(1.2\text{–}1.0) \times 10^{-3}$ K^{-1} slope of the $\Delta f_A/\Delta T$ relation.

4. Discussion

4.1. Comparison of the behavior of Fe-FER and Fe-MFI samples

The structures of FER and MFI frameworks are similar: they have the same a–b planes, the channels in direction c are different [10]. Thus, similar behavior is expected, since the Mössbauer effect is primarily sensitive to the near vicinity of the probe nucleus. Indeed, the expected similarity was manifested: both the reversible redox behavior upon hydrogen treatment and the insensitivity of average Θ_D to the treatments were characteristic for the two samples.

However, the Fe-MFI sample additionally exhibited autoreduction of Fe^{3+} to the Fe^{2+} state already upon evacuation, not shown by the Fe-FER sample. The appearance of the autoreduction can probably be interpreted by the presence of extra-framework iron in higher proportions in the Fe-MFI. This sample was calcined at 973 K, and this high-temperature treatment resulted in partial loss of framework iron [22]. The mixed presence of extra-framework and framework iron may lead to autoreduction (and further removal of iron from the framework) [15,16].

4.2. Reversible redox behavior and centers of oxygenation

In catalytic oxygenation processes probably the reversible redox feature plays a primary role. This feature was exhibited in two senses by both the Fe-FER and Fe-MFI

samples upon hydrogen treatment. First, an Fe^{2+} state was stabilized at 77 K, the major part of which disappeared simply by raising the measuring temperature to 300 K. The appearance of this temporary state was assigned to the lesser stability of the reduced state in the $Fe_{framework}$–O–$Fe_{extra\text{-}framework}$ centers [14]. Second, the reduction cycle could be repeated by the following hydrogen treatment with only minor structural rearrangements (a slight loss of iron from the framework was detected). The Fe-FER sample exhibits catalytic activity, and – based on the same behavior and very similar structure – the existence of the same $Fe_{framework}$–O–$Fe_{extra\text{-}framework}$ dinuclear centers can be proposed for Fe-MFI, as well.

It is worth mentioning that the appearance of the redox feature can still be observed if the sample contains a certain portion of iron in extra-framework positions, as was the case for the latter Fe-MFI sample (although the effect is attributed to mixed $Fe_{framework}$–O–$Fe_{extra\text{-}framework}$ dinuclear pairs). Further on, it should also be added that associated, fully extra-framework ions do not display the reversible redox behavior: once they are reduced they remain in the Fe^{2+} state – as was proved, for example, in [25,26].

4.3. Bonding strength: analysis of RAA and Debye temperature data

Similarly to the reversible redox behavior, the data obtained for the resonant absorption area, RAA, and Debye temperature, Θ_D, showed similar features for both samples. As for the RAA values, they hardly depended upon the treatment. This suggests that each component contributed similarly to the spectra regardless of the different conditions applied. Even in the cases of hydrogen treatments in which the $Fe^{3+} \rightarrow Fe^{2+}$ reduction has taken place in a fairly large extent (37 and 51% presence of Fe^{2+}, as the RI values reflect for MFI and FER), only a modest change (max. 15%) is found in the RAA values. This observation suggests that the change in the oxidation state is not connected necessarily with simultaneous removal of ions from the framework, the major part of the Fe^{2+} component formed still remains bonded.

Evaluation of average Θ_D values ($260 < \Theta_D < 300$ K) estimated from the $\Delta f_A/\Delta T$ slopes allows one to estimate a medium bond strength for the iron species. For example, in bulk oxides (e.g., in ferrates) $\Theta_D = 514$ and 425 K were determined for Fe^{3+}_{Td} and Fe^{3+}_{Oh}, respectively [17]. On the other hand (e.g., for Fe^{2+} in phthalocyanine complexes encapsulated in zeolite cages [27], or for Fe^{3+} coordinated by adsorbed water [19]) $\Theta_D \approx 150$ K can be estimated from the data reported. Thus, the recently estimated 260–300 K reflects a medium strength bonding state. This value provides further, indirect support for the previously suggested $Fe_{framework}$–O–$Fe_{extra\text{-}framework}$ emplacement where the stiffer framework position is combined with that of the looser extra-framework in significant portions of iron in both the FER and MFI samples.

4.4. Considerations related to other properties of Fe-FER and Fe-MFI catalysts

Interpretation of certain other properties of the Fe-MFI catalysts can also be suggested in agreement with the above presented considerations. First, the stability of the catalyst is probably related to the partial attachment of the dinuclear center to the framework. On the one hand, since the migration of the center inside the channels is hindered, the formation of larger associated iron oxide clusters is blocked (which would result in loss of catalytic activity). On the other hand, the partially fixed dinuclear center is flexible enough to absorb the size change in the ionic radii (Fe^{3+} 64 pm, Fe^{2+} 74 pm) in the redox process, without being removed from the framework.

Another related point is the variety of possible preparation routes. As was mentioned, effective catalysts can be pepared either by ion exchange (solid state or in aqueous media), or by isomorphous substitution in the primary synthesis. The partial attachment of the dinuclear centers can easily be achieved by virtue of the iron species introduced in the ion exchange: e.g., the vapor of $FeCl_3$ is composed of Fe_2Cl_6 (in cases [3,4]) or, in aqueous media, dinuclear species are present even at low pH values [22]. These dinuclear entities can be attached to –OH groups or to defect sites, particularly if the starting zeolite contains framework Al as well (cases [1–5]), further calcination stabilizes the centers. (Contrasting examples can also be found, when the introduced iron-containing molecules do not sufficiently interact with the framework, e.g., iron oxalate proved to be a poor precursor for ion exchange peparation both for Y [28] and for certain MFI catalysts [29].)

A similar explanation may hold for the iron component introduced already at the starting synthesis: the dinuclear iron centers are primarily present in the synthesis gel (the very low pH would destroy the structure) and the dinuclear centers are probably already incorporated in the process of the synthesis [22]. In addition, centers may be formed during the catalytic reactions as well, when an extra-framework iron species (e.g., FeO^+) migrates to the Brønsted acidic $Fe^{3+}_{Td,2}$ framework site and a dinuclear center is formed by replacing the proton in the Si–O–Fe(OH)–O–Si group for the migrating species.

5. Conclusion

Both Fe-FER and Fe-MFI demonstrated similar behavior in redox processes. Reversibility can be found in two senses: in the temporary appearance of an Fe^{2+} state and in the possibility of cycling of the catalyst without significant rearrangement of Fe ions. Together with the reversible redox behavior medium values can be estimated for the average Debye temperature ($260 < \Theta_D < 300$ K). The medium value for Θ_D provides an additional support for the partial attachment of certain iron species to the framework. Thus, the extension of the explanation suggested previously for

the Fe-FER catalyst (viz. the catalytic role of $Fe_{framework}$–O–$Fe_{extra\text{-}framework}$ pairs) is proposed for Fe-MFI as well. Other properties of the ferrisilicate catalysts (stability and variety in the ways of preparation) can also be interpreted by the concept outlined here.

Acknowledgement

The financial support provided by the Hungarian National Science Research Fund (under OTKA projects T014873 and T021131) is gratefully acknowledged.

References

[1] X. Feng and W.K. Hall, Catal. Lett. 41 (1996) 45.
[2] X. Feng and W.K. Hall, J. Catal. 166 (1997) 368.
[3] H.-Y. Chen and W.M.H. Sachtler, Catal. Lett. 50 (1998) 125.
[4] H.-Y. Chen and W.M.H. Sachtler, Catal. Today 42 (1998) 73.
[5] M. Kögel, V.H. Sandoval, W. Schwieger, A. Tissler and T. Turek, Catal. Lett. 51 (1998) 23.
[6] S. Iwamoto, S. Kon, S. Yoshida and T. Inui, Stud. Surf. Sci. Catal. 105 (1997) 1587.
[7] G.I. Panov, A.K. Uriarte, M.A. Rodkin and V.I. Sobolev, Catal. Today 41 (1998) 365.
[8] G.I. Panov, V.I. Sobolev, K.A. Dubkov, V.N. Parmon, N.S. Ovanesyan, A.E. Shilov and A.A. Shteinman, React. Kinet. Catal. Lett. 61 (1997) 251.
[9] Md.A. Uddin, T. Komatsu and T. Yashima, J. Catal. 150 (1994) 439.
[10] C.L. Kibby, A.J. Perrotta and F.E. Massoth, J. Catal. 35 (1974) 256.
[11] S. Shevade, R.K. Ahedi and A.N. Kotasthane, Catal. Lett. 49 (1997) 69.
[12] R.W. Joyner and M. Stockenhuber, Catal. Lett. 45 (1997) 15.
[13] R. Schmidt, M.D. Amiridis, J.A. Dumesic, L.M. Zelewski and W.S. Millman, J. Phys. Chem. 96 (1992) 8142.
[14] K. Lázár, G. Lejeune, R.K. Ahedi, S. Shevade and A.N. Kotasthane, J. Phys. Chem. B 102 (1998) 4865.
[15] J. Novakova, L. Kubelkova, B. Wichterlowa, T. Juska and Z. Dolejsek, Zeolites 2 (1982) 17.
[16] P.A. Jacobs, Stud. Surf. Sci. Catal. 29 (1986) 357.
[17] L. Fournes, Y. Potin, J.C. Grenier and P. Hagenmuller, Rev. Phys. Appl. 24 (1989) 463.
[18] J.W. Niemantsverdriet, A.M. van der Kraan and W.N. Delgass, J. Catal. 89 (1984) 138.
[19] W.N. Delgass, R.L. Garten and M. Boudart, J. Chem. Phys. 50 (1969) 4603.
[20] K. Lázár, A. M.-Szeleczky, N.K. Mal and A.V. Ramaswamy, Zeolites 19 (1997) 123.
[21] P. Fejes, J.B. Nagy, K. Kovács and G. Vankó, Appl. Catal. A 145 (1996) 155.
[22] P. Fejes, J.B. Nagy, J. Halász and A. Oszkó, Appl. Catal. A 175 (1998) 89.
[23] R.G. Burns, Hyperfine Interact. 91 (1994) 739.
[24] A. Meagher, V. Nair and R. Szostak, Zeolites 8 (1988) 3.
[25] K. Lázár, G. Borbély and H. Beyer, Zeolites 11 (1991) 214.
[26] K. Lázár, A. M.-Szeleczky, G. Vorbeck, R. Fricke, A. Vondrova and J. Cejka, J. Radioanal. Nucl. Chem. 190 (1995) 407.
[27] K. Lázár, A. M.-Szeleczky, F. Notheisz and Á. Zsigmond, Stud. Surf. Sci. Catal. 94 (1995) 720.
[28] K. Lázár, G. Pál-Borbély, H.K. Beyer and H.G. Karge, Stud. Surf. Sci. Catal. 91 (1995) 551.
[29] W.K. Hall, X. Feng, J. Dumesic and R. Watwe, Catal. Lett. 52 (1998) 13.